ANNEXURE

Nickel salt phosphomolybdic acid ($NiHPMo_{12}$): Synthesis, characterization and application for oxidative esterification

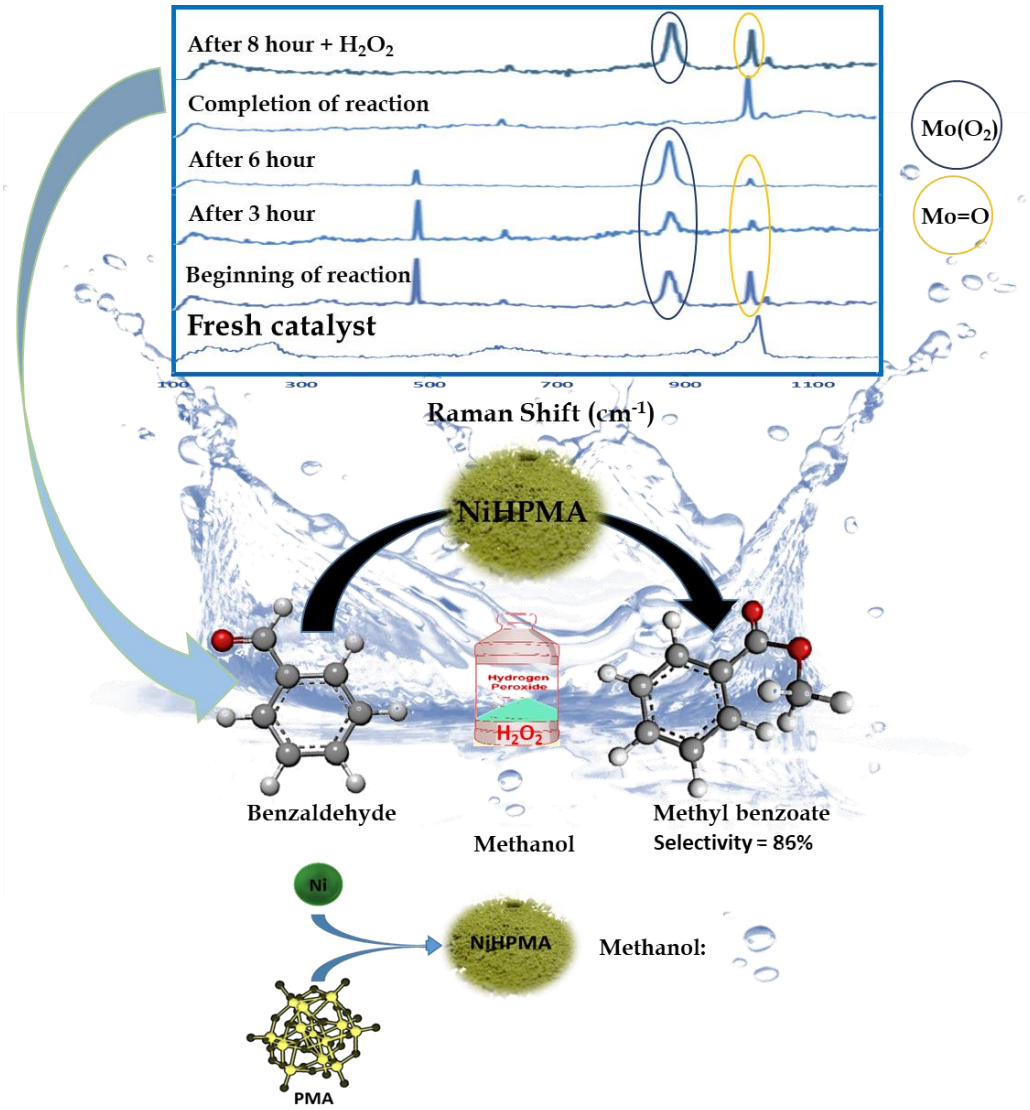

RSC Advances

PAPER

Check for updates

Cite this: *RSC Adv.*, 2020, **10**, 22146

Nickel salt of phosphomolybdic acid as a bi-functional homogeneous recyclable catalyst for base free transformation of aldehyde into ester†

Anjali Patel * and Jay Patel

A Ni salt of phosphomolybdic acid (NiHPMA) was synthesized and characterized by various physico-chemical techniques such as EDX, UV-Visible spectroscopy, FT-IR, Raman spectroscopy and XPS. FT-IR and Raman spectroscopy confirm the presence of Ni as a counter cation while UV-Visible and XPS studies to confirm the presence of Ni(II) in the catalyst. The catalyst was evaluated for its bi-functional activity towards the tandem conversion of benzaldehyde to ethyl benzoate and it was found that very small amounts of Ni (2.64×10^{-3} mmol) enhance the selectivity towards benzoate. A detailed mechanistic study was carried out by UV-Visible and Raman spectroscopy to confirm that both intermediate species, Mo–peroxo and Ni–oxo, are responsible for higher selectivity towards esters. Further, a study to determine the effect of addenda atoms (heteropoly acid) was also carried out. The catalyst was also found to be viable for a number of aldehydes under optimized conditions.

Received 7th May 2020
Accepted 29th May 2020

DOI: 10.1039/d0ra04119j

rsc.li/rsc-advances

Over the last four decades, metal salt of polyoxometalate (MSPOMs) have gained tremendous attention as catalysts because they combine the advantage of both polyoxometalate (POMs) as well as metal.

It is well known that POMs possess a very strong acidity in form of protons, which can be changed by varying the chemical composition of the primary structure of the POMs anion [1] as described in general introduction. These exchangeable protons can be easily replaced by other cations, without affecting the primary structure [2, 3]. Depending on the nature of cations (i.e. salt of POMs), acidic/redox properties can be tuned, which makes them important catalytic materials for various organic transformations [4-6]. Amongst, transition metal salt of phosphotungstic acid and silicotungstic acid are studied in details and a number of reports are available for the same. At the same time, studies on transition metal salt of phosphomolybdic acid are comparatively less. In this context, articles on first row of 3d transition metal salts (V, Fe, Co, Ni, Cu and Zn) of PMo_{12} are reported [6-21]. Out of those reported articles, only five articles are available on Ni salt of PMo_{12} even though Ni is well-known for the its Lewis acidy.

In 1974, Tsigdions [17], first time, reported the synthesis of $Ni_3[PMo_{12}O_{40}]_2.34H_2O$ and studied their thermal behavior, solubility and hydrolytic strength in different solvents mixture including aqueous medium. After almost two decades, in 1994, Mizuno et al. [18] reported synthesis of $Cs_{2.5}Ni_{0.08}H_{0.34}PMo_{12}O_{40}$ and its use for oxidation of isobutene to methacrylic acid and methacrolein using molecular O_2. In 1999, Demirel et al. [14] reported liquefaction of wyodak coal using same catalyst, reported by Tsigdions [17]. Later, in 2010, Rabia et al. [19] reported synthesis of $(NH_4)_xM_yH_zPMo_{12}O_{40}$ (M = Ni^{2+}, Co^{2+} or Fe^{3+}) using same method as Mizuno et al. reported [18] and catalytic activity for oxidation of propane. In 2015, the same group came up with the use of soluble $H_{3-2x}Ni_xPMo_{12}O_{40}$ and $(NH_4)_{3-2x}Ni_xPMo_{12}O_{40}$ where x: 0.25 – 1.5 for oxidation of cyclohexanone to adipic acid [20]. Further in 2019, same group [21]

synthesized a series of transition metal salt of phosphomolybdic acid [$HMPMo_{12}O_{40}$ (M:Co, Ni, Mn, Cu or Zn)] by using their own method and described their use as catalysts for the synthesis of adipic acid from cyclohexanone.

Above literature survey shows (i) Oxidative esterification was not at all studied (iii) although nickel salt of phosphomolybdic acid is excellent and sustainable for the oxidation reaction, full characterization of the same is missing and no single report is available for any tandem reaction to show the bi-functional effect of Ni as well as Mo.

Tandem oxidative esterification reaction is selected as one of the best example of tandem reaction. Oxidative esterification of aldehydes with alcohols has received huge attention during recent years because it produces ester which are abundantly used as industrial raw materials. Methyl esters play a significant role in chemical industries, including the flavoring agents, fragrance industry, diluents, solvent extractants and intermediates [22, 23]. The traditional method for synthesizing ester involves two steps: first, the aldehyde is oxidized using manganese dioxide or sodium dichromate, and then the intermediate carboxylic acid is further converted into methyl ester. These methods have limitations since chemical processes produce a significant amount of harmful wastes and byproducts. The development of the direct synthesis of esters from the oxidative esterification of aldehydes with alcohols, where two reaction steps take place in a single step, has received a lot of attention in recent years. This approach can be a significant improvement over conventional approaches in terms of green, economical, and sustainable chemistry because it only requires one step of reaction and produces no byproducts.

Taking into consideration of the advantages of tandem reaction as well as Lewis acidity of Ni and redox ability of Mo, in this chapter, we report synthesis of Ni salt of phosphomolybdic. This was followed by first time detailed characterization of the synthesized catalyst by EDX, TGA, UV-Vis, FT-IR, Raman

spectroscopy, and XPS along with catalytic evaluation for tandem oxidative esterification of benzaldehyde to ester. The reaction was carried out using methanol and H_2O_2 and various reaction parameters such as catalyst amount, amount of H_2O_2, the volume of methanol, reaction time and reaction temperature were optimized for maximum conversion as well as selectivity towards ester. The recycling and reusability of synthesized catalyst was carried out up to three cycles. Detailed reaction mechanism was proposed based on Raman and UV-visible spectroscopy studies.

EXPERIMENTAL

Materials

All chemicals used were of A. R. grade. Phosphomolybdic acid, nickel acetate, benzaldehyde, methanol, 30% hydrogen peroxide (H_2O_2) V/V and dichloromethane obtained from Merck were used as received.

Catalyst synthesis

Nickel salt of phosphomolybdic acid was synthesized by direct method as reported in the literature [24] with modification. A saturated solution of nickel acetate (0.1244 g, 0.5 mmol) was added drop wise into solution of $H_3PMo_{12}O_{40}$ (0.9126 g, 0.5 mmol) dissolved in a minimum amount of water. The resulting mixture was aged for 1 h at 80 ^{0}C and excess of water was evaporated on water bath. The obtained material was dried at 100 ^{0}C for 10 hours and calcined at 300 ^{0}C under air atmosphere for 2 h in a muffle furnace. The resulting green color, material was designated as $NiHPMo_{12}$. The synthetic scheme of $NiHPMo_{12}$ is shown in scheme 1.

To see any decomposition, $HPMo_{12}O_{40}$ was also calcined under the same conditions and it was found that color remains yellow, good agreement with the reported literature [25].

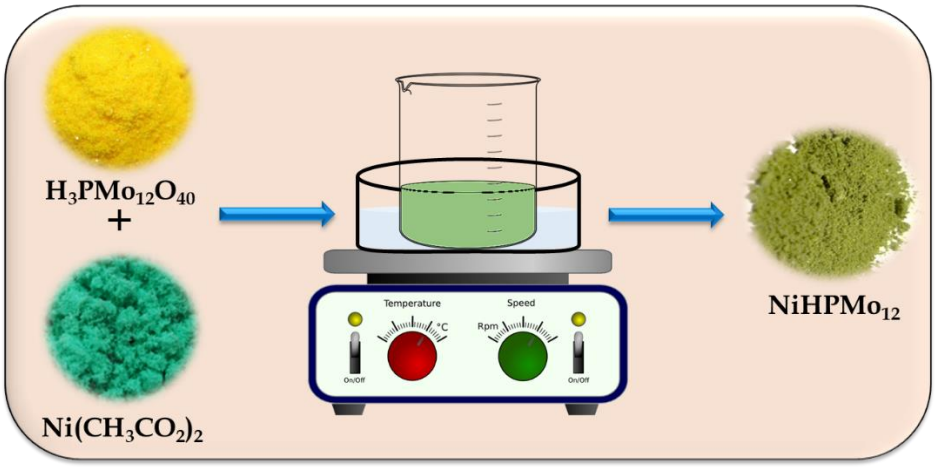

Scheme 1. Synthesis of $NiHPMo_{12}$

Catalytic activity

For oxidative esterification of benzaldehyde, 50 ml glass batch reactor provided with a double walled air condenser, magnetic stirrer and guard tube. The glass batch reactor was charged with benzaldehyde (10 mmol) with H_2O_2 (30 mmol, 30% H_2O_2 v/v), methanol (7 mL), catalyst (5 mg) and stirred at 80 ^oC for 6 h. After completion of reaction, mixture was extracted with dichloromethane. The organic phases were then dried with anhydrous magnesium sulfate and analyzed by GC. The obtained products were identified by comparison with the authentic samples. The %conversion and %selectivity of product was calculated using equation as mentioned in general introduction. The schematic representation for the catalytic methodology is presented in scheme 2.

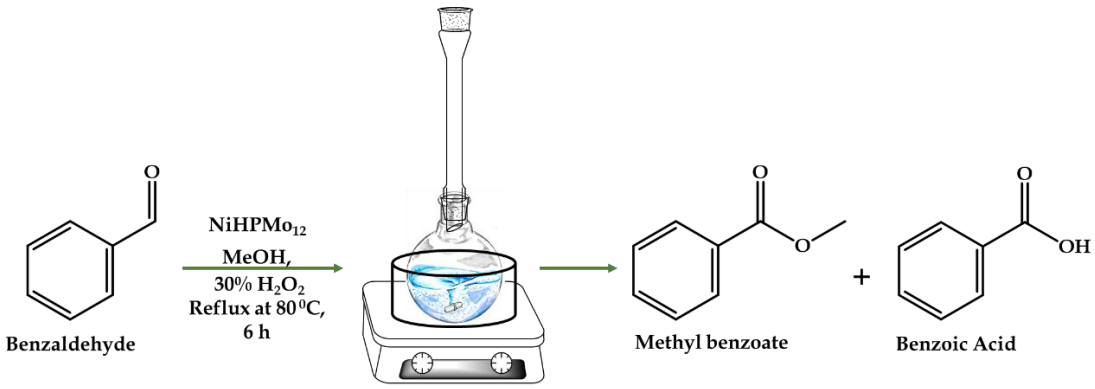

Scheme 2. schematic representation of oxidative esterification reaction

RESULT AND DISCUSSION

Characterization

The EDX mapping of $NiHPMo_{12}$ (Figure 1) shows that presence of all expected elements (Ni, P, Mo and O). The ascertained EDX values of all the elements are in good agreement with the theoretical values. EDX values (% wt): Ni, 2.89; Mo, 57.15; P, 1.39; O, 38.57) and calculated values (% wt): Ni, 2.92; Mo, 57.34; P, 1.54; O, 38.20).

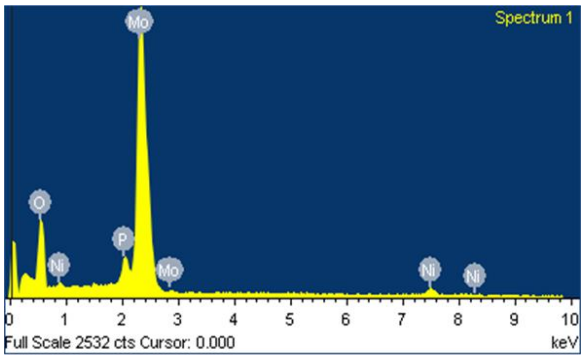

Figure 1. EDX mapping of $NiHPMo_{12}$

TGA of $NiHPMo_{12}$ shows (Figure 2) initial weight loss of 2.46 % up to 100 ^{o}C, due to the removal of adsorbed water. Further, it shows 4.11 % weight loss up to 280 ^{o}C corresponding to removal of water of crystallization. Further, no appreciable weight loss was noticed, indicating the thermal stability of the synthesized material up to 500 ^{o}C. Based on the total weight loss, the number of water molecule was calculated using the formula same formula as mentioned in part A chapter 1 and it was found to be 6. From the EDX and TGA, the chemical formula of the synthesized material is proposed as $NiH[PMo_{12}O_{40}].6H_2O$.

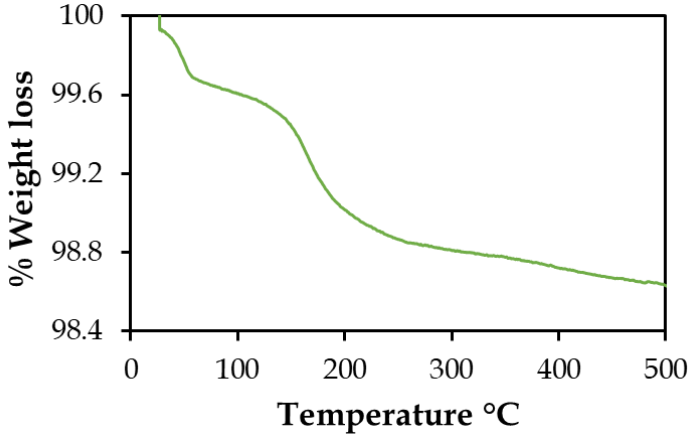

Figure 2. TGA of $NiHPMo_{12}$

The UV-visible spectrum of $NiHPMo_{12}$ shows (Figure 3) the absorption peak at 230 nm due to the charge transfer between $O^{2-} \rightarrow Mo^{6+}$ [26]. In addition, it also shows an absorption peak at 396 nm, corresponding to the presence of Ni(II) [22] which is the first indication of the presence of Ni in the synthesized materials.

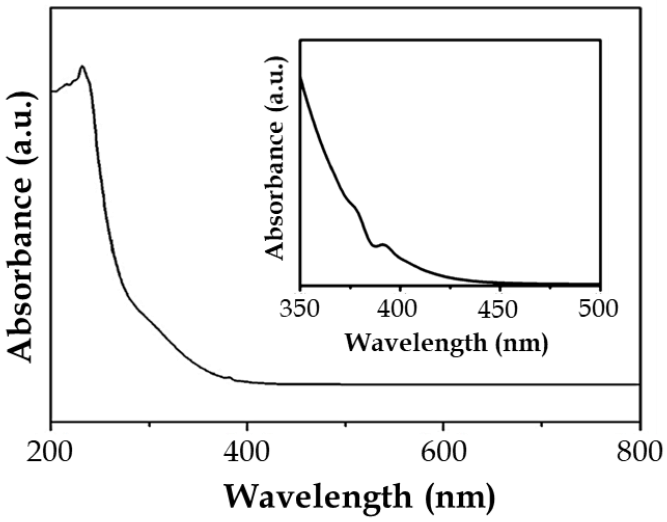

Figure 3. UV-Visible spectra of $NiHPMo_{12}$

The FT-IR spectra of PMo_{12} shows (Figure 4) the characteristic bands at 1070, 965, 870 and 790 cm^{-1} corresponding to stretching vibration of P-O, $Mo=O_t$, $Mo–O_b–Mo$ and $Mo-O_c-Mo$ respectively [27, 28]. Whereas $NiHPMo_{12}$ shows all characteristic bands without any significant shift at 1070, 960, 871 and 786 cm^{-1} corresponding to stretching vibrations of P-O, $M=O_t$, $Mo-O_b-Mo$ and $Mo-O_c-Mo$ respectively and with an additional band at 455 cm^{-1}, a characteristic peak of (Ni-

O) bond indicating the presence of Ni [20, 21]. Moreover, the presence of P-O stretching is at exactly same wavelength (1070 cm^{-1}) confirming the presence of Ni as counter cation only, via exchange of available protons of PMo_{12}.

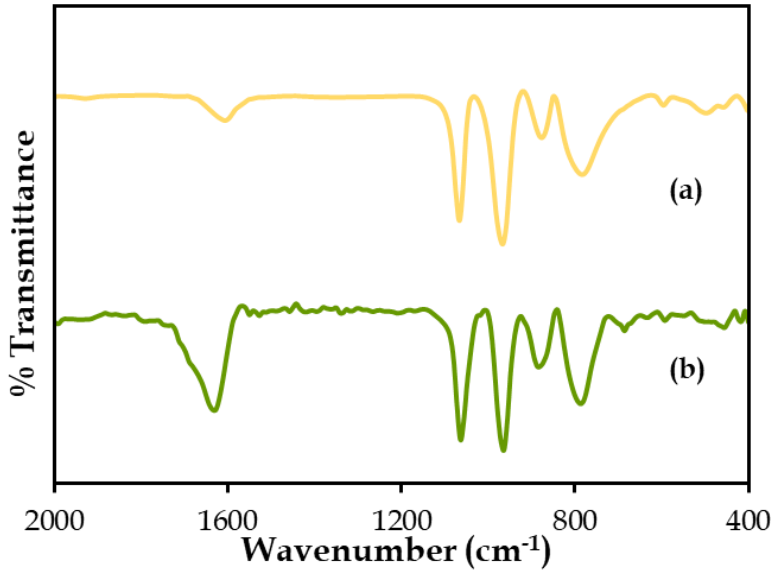

Figure 4. FT-IR spectra of (a) PMo_{12} and (b) $NiHPMo_{12}$

The Raman spectra of PMo_{12} was recorded (Figure 5a) and is in good agreement with the reported one [29, 30]. The Raman spectra of $NiHPMo_{12}$ show (Figure 5b) peaks with slight shifting at 1004, 980, 973, 913, 609, and 295 cm^{-1} for v_s ($Mo=O_t$), v_{as} ($Mo-O_t$), v_s (P-O), v_{as} ($Mo-O_b-Mo$), v_s ($Mo-O_b-Mo$) and v_s ($Mo-O_a$) vibration respectively [31].The observed shifting in all the characteristic bands may be due to change in the environment because of the exchange of available protons of PMo_{12} by Ni.

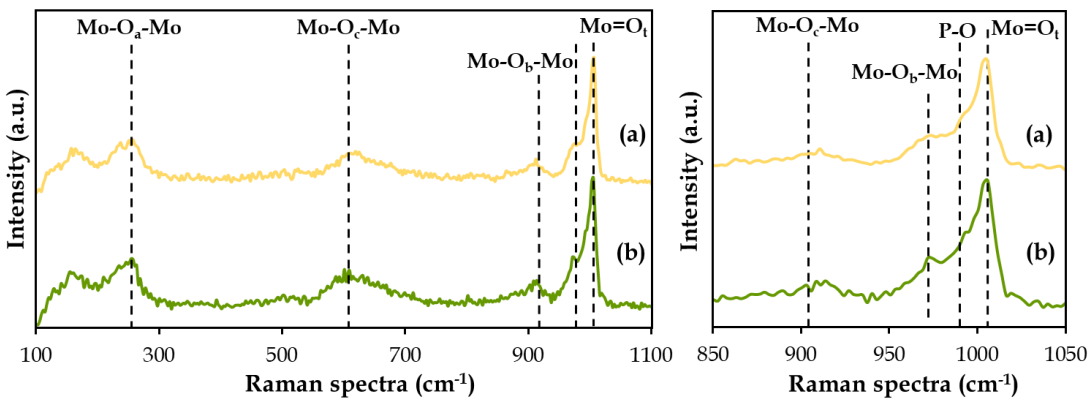

Figure 5. Raman spectra of (a) PMo_{12} and (b) $NiHPMo_{12}$

The XPS of $NiHPMo_{12}$ shows (Figure 6) that intense peaks at 233, 397 and 416 eV corresponds to 3d3/2, 3p3/2 and 3p1/2 respectively and low intense peak at 235 eV corresponds to 3d3/2 energy level of Mo(VI) [32, 33]. Furthermore, the peak at 871 eV with lower intensity corresponds to $2p_{1/2}$ energy level of Ni(II) which is in good agreement with reported ones [34-36]. However, low intensity of peak of Ni can be attributed to low concentration of Ni (2.64×10^{-3} mmol) in the synthesized material.

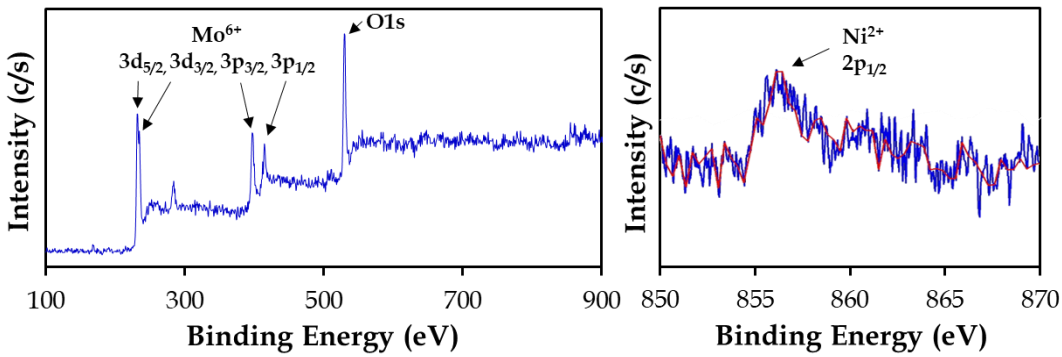

Figure 6. XPS spectra of $NiHPMo_{12}$

Catalytic Activity

Oxidative esterification was selected as a model reaction for evaluation of catalyst efficiency and for this benzaldehyde and methanol (MeOH) were used as test substrates in the presence of hydrogen peroxide as an oxidant (scheme 2). The effect of various reaction parameters such as catalyst amount, MeOH volume, substrate to H_2O_2 ratio, time and temperature were studied to optimize the conditions for maximum conversion as well as selectivity towards the ester. Each experiment was carried out thrice and the results obtained were reproducible with an error of ±1-1.5%.

To evaluate the effect of H_2O_2, the reaction was carried out with different mole ratio of benzaldehyde to H_2O_2 by keeping all other parameters constant. Obtained result shows that on increasing the amount of oxidant from 10 mmol (1:1) to 40 mmol (1:4), conversion also increases which is in good agreement with chemical dynamics [36, 37], indicating that the oxidative esterification could be

improved by increasing the amount of H_2O_2. Concurrently, the selectivity towards desired product, methyl benzoate, decreases because the higher amount of oxidant will tolerate more oxidation of benzaldehyde to convert into benzoic acid. Hence 1:3 ratio of substrate to H_2O_2 was optimized.

Table 1. Effect of H_2O_2

Styrene: H_2O_2 (mmol)	% Conversion	% Selectivity	
		Ester	Acid
10: 10	51	96	04
10: 20	62	88	12
10: 30	68	86	14
10: 40	74	64	36

Reaction conditions: catalyst (5 mg), benzaldehyde (10 mmol), oxidant (30% H_2O_2 v/v), MeOH (7 mL), temperature (80 ^{0}C) and time (6 h).

The effect of catalyst amount was studied by varying the amount from 5 to 20 mg. The obtained results are shown in Figure 7a. On increasing the amount of catalyst from 5 to 20 mg, decrease in % conversion as well as % selectivity of ester was observed due to the unproductive decomposition of H_2O_2 in the presence of excess catalyst which generates additional water, shifting the equilibrium towards left and hence the decrease in conversion, which is in good agreement with the reported one [23]. Therefore, 5 mg of catalyst amount was optimized for maximum 68 % conversion with highest selectivity (86 %) towards ester.

The effect of MeOH amount was investigated in the range of 4 to 8 mL (Figure 7b). Obtained results shows that on increasing volume of MeOH, % conversion decreased and selectivity of ester increased up to 7 mL, which may be due to dilution of substrate with MeOH. Hence, 7 mL of MeOH was optimized from the obtained results.

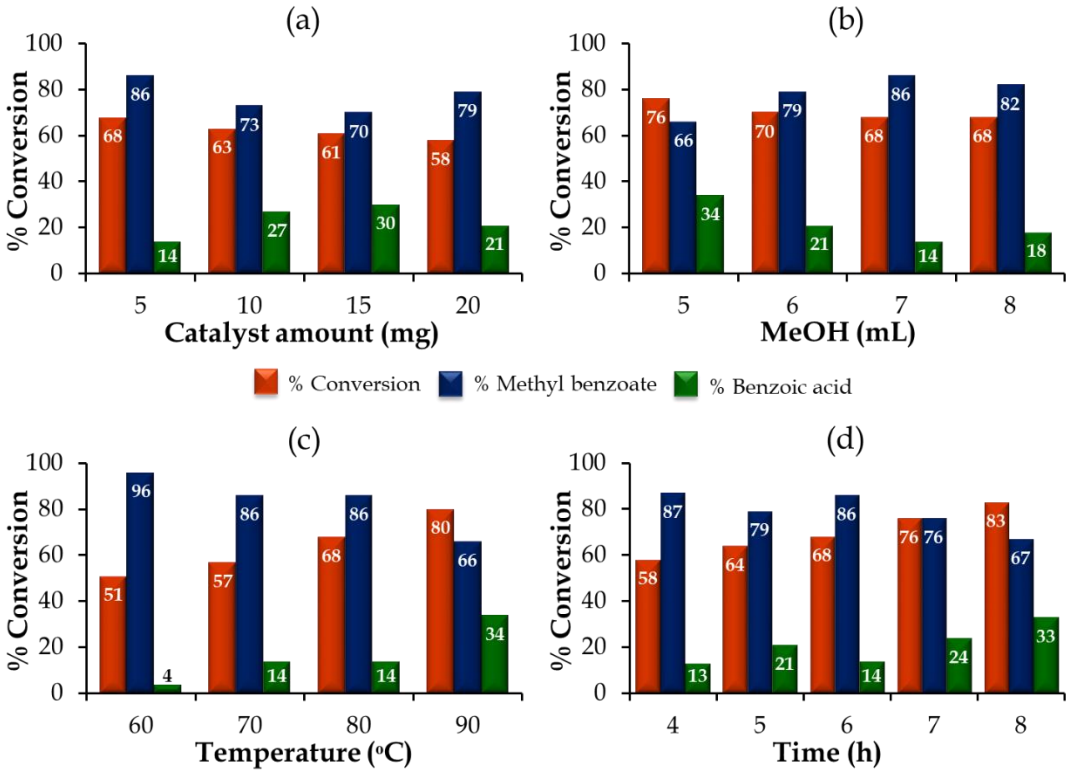

Figure 7. Optimization of parameters for oxidative esterification of benzaldehyde. Reaction conditions: (a) Effect of catalyst amount- benzaldehyde (10 mmol), H_2O_2 (30 mmol, 30% H_2O_2 v/v), MeOH (7 mL), temperature (80 ^{0}C) and time (6 h); (b) effect of MeOH- catalyst (5 mg), benzaldehyde (10 mmol), H_2O_2 (30 mmol, 30% H_2O_2 v/v), temperature (80 ^{0}C) and time (6 h); (c) Effect of temperature: catalyst (5 mg), benzaldehyde (10 mmol), H_2O_2 (30 mmol, 30% H_2O_2 v/v), MeOH (7 mL) and time (6 h); (d) Effect of time: catalyst (5 mg), benzaldehyde (10 mmol), H_2O_2 (30 mmol, 30% H_2O_2 v/v), MeOH (7 mL) and temperature (80 ^{0}C).

The effect of temperature was screened between the range of 60 to 90 ^{0}C. The obtained results show (Figure 7c) that on increasing reaction temperature up to 90 ^{0}C, conversion increased and the selectivity towards ester decreased because of thermal and catalytic decomposition of H_2O_2 at high temperature [23, 36]. Therefore, 80 ^{0}C was optimized.

The effect of reaction time was monitored between ranges of 4 to 8 h (Figure 7d). Obtained results display that as reaction time increases, conversion also increases but the selectivity of ester decreases which is due to decomposition of H_2O_2 generated water molecule, which leads to hydrolysis of ester to aldehyde.

The optimized condition for maximum 68% conversion with highest 86% selectivity are: catalyst (5mg), active amount of Ni (0.155 mg), benzaldehyde (10 mmol), catalyst/substrate ratio (2.64×10^{-4}), 30% H_2O_2 v/v (30 mmol), MeOH (7 mL), temperature (80 ^{0}C) and time (6 hour) with TON (2576).

The chromatographs of optimized reaction condition for oxidative esterification of benzaldehyd*e* are shown in figure 8.

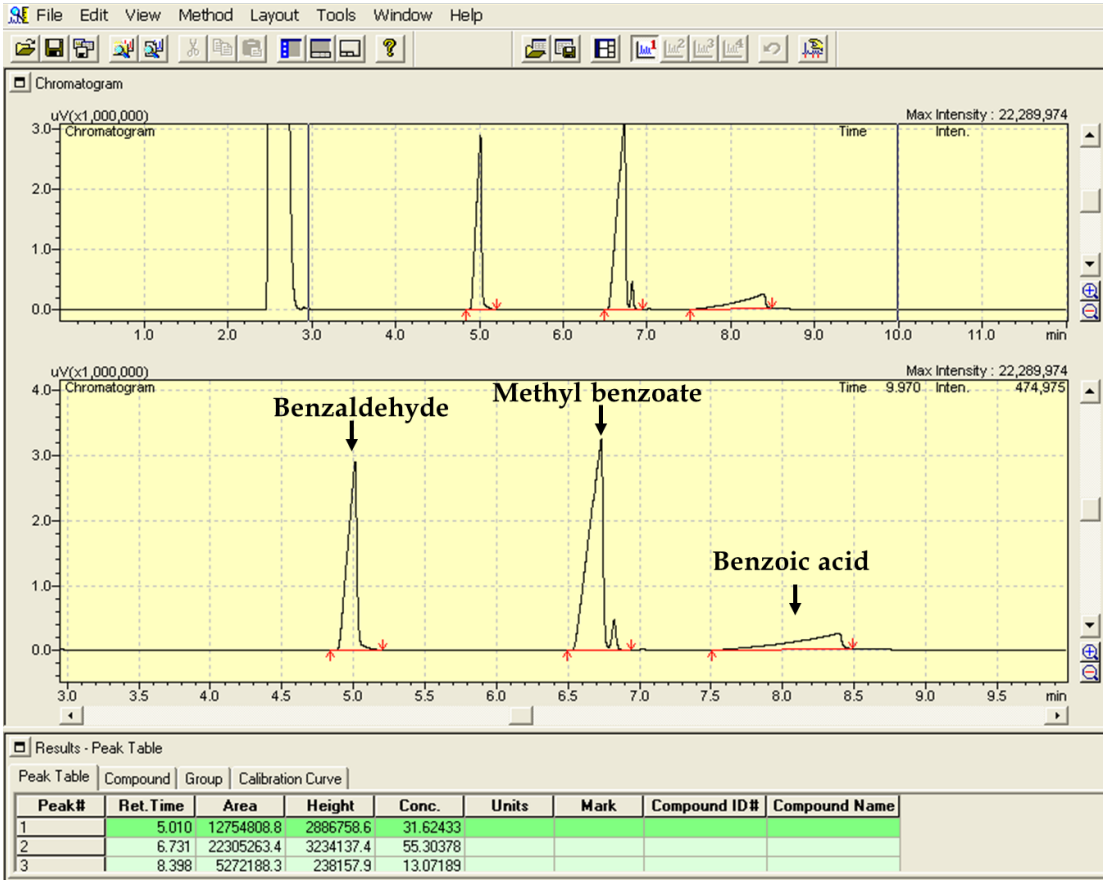

Figure 8. Gas chromatograph of benzaldehyde oxidative esterification

Control experiment and effect of addenda atom

In control experiments, the reaction was carried out with $Ni(CH_3COO)_2$ and PMo_{12} in optimized experimental conditions and obtained results are shown in table 2. In case of $Ni(CH_3COO)_2$, 49% conversion was obtained with 64% selectivity of ester because of the Lewis acidity of Ni, whereas in case of PMo_{12}, 46% conversion was achieved with 67% ester selectivity. Furthermore, when the

reaction was carried out with $NiHPMo_{12}$, 68 % conversion with 86 % selectivity towards ester was achieved due to Ni increased Lewis acidity and total acidity of catalyst which enhance selectivity of ester. The obtained result indicates the bi-functional nature of catalyst where Mo contributes for oxidation and Ni for esterification due to its Lewis acidity.

Table 2. Control experiment

Catalyst	% Conversion	% Selectivity	
		Ester	Acid
$Ni(CH_3COO)_2$	49	64	36
PMo_{12}	46	67	33
$NiHPMo_{12}$	68	86	14
$NiHPW_{12}$	45	97	03

Reaction conditions: catalyst (Ni: 0.155 mg), benzaldehyde (10 mmol), oxidant (30% H_2O_2 v/v), methanol (7 mL), temperature (80 ^{0}C) and time (6 h).

In order to see the effect of an addenda atom, the catalytic activity of Ni salt of Phosphotungtic acid ($NiHPW_{12}$) was also evaluated for the said reaction under same experimental conditions and obtained results are presented in table 2. It is very interesting to note that the trend exactly follows the known order of acidity and redox ability of different POMs.

Order of acidity: Phosphotungstic acid (PW_{12}) > Silicotungstic acid (SiW_{12}) > Phosphomolybdic acid (PMo_{12}) > Silicomolybdic acid ($SiMo_{12}$)

Order of redox ability: Phosphomolybdic acid (PMo_{12}) > Silicomolybdic acid ($SiMo_{12}$) > Silicotungstic acid (SiW_{12}) > Phosphotungstic acid (PW_{12})

As the PMo_{12} has maximum oxidation ability, it will give more conversion (as per the proposed mechanism, Mo-peroxo is responsible for oxidation), while being a most acidic PW_{12} will contribute more towards the formation of the ester in addition to Ni (Lewis acidity).

Role of each substrate

To know the role of each substrate (table 3), various experiments were carried out: (i) without catalyst (benzaldehyde + MeOH + H_2O_2) the reaction proceed to give negligible conversion, which indicates the requirement of an efficient catalyst for the fast reaction (ii) without H_2O_2 (catalyst + MeOH + benzaldehyde) the reaction did not show significant conversion (iii) without MeOH (catalyst + benzaldehyde + H_2O_2), gives 100% conversion with single selective product benzoic acid. This study indicates that all three components; catalyst, MeOH and H_2O_2 are essential for the oxidative esterification reaction.

Table 3. Role of substrate

Catalyst	% Conversion	% Selectivity	
		Ester	Acid
Without catalyst (benzaldehyde + MeOH + H_2O_2)	4	-	100
Without H_2O_2 (catalyst + MeOH + benzaldehyde)	15	76	24
Without MeOH (catalyst + benzaldehyde + H_2O_2)	45	-	100

Reaction conditions: catalyst (5 mg), catalyst/substrate ratio (2.64×10^{-4}), benzaldehyde (10 mmol), oxidant (30 mmol, 30% H_2O_2 v/v), MeOH (7 mL), temperature (80 ^{0}C) and time (6 h).

Regeneration and recycling of catalyst

After completion of reaction, the reaction mixture was cooled to room temperature and organic layer was extracted by dichloromethane (DCM). The aqueous phase was dried at 100 ^{0}C to recover the homogeneous solid catalyst. The similar procedure was followed up to three cycles.

The obtained results, with the regenerated catalyst in optimized identical conditions, show (Table 4) no significant change in % conversion as well as %

selectivity of ester up to three cycles. Obtained result indicates that during the reaction the catalyst remains stable, and can be reused over multiple cycles.

Table 4. Catalyst reusability

Catalyst	% Conversion	% Selectivity	
		Ester	Acid
Fresh	68	86	14
Cycle – 1	67	84	16
Cycle – 2	67	84	16
Cycle - 3	67	84	16

Reaction conditions: catalyst (5 mg), benzaldehyde (10 mmol), oxidant (30 mmol, 30% H_2O_2 v/v), MeOH (7 mL), temperature (80 ^{0}C) and time (6 h).

Characterization of regenerated catalyst

Regenerated catalyst was characterized by EDX, FT-IR, UV-visible and XPS for the confirmation of prevention of catalyst structure.

EDX mapping shows (Figure 9) the presence of Ni, P, Mo and O in the regenerated catalyst. The obatined EDX wt% is (Ni, 2.93; Mo, 57.35; P, 1.39; O, 38.58) are in good agreement with a fresh one.

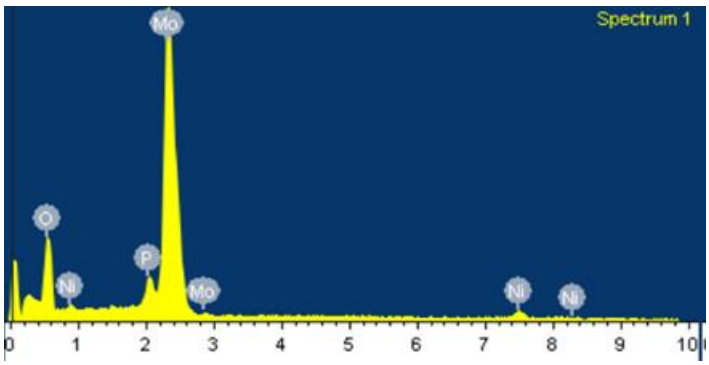

Figure 9. EDX mapping of regenerated $NiHPMo_{12}$

The FT-IR spectra of regenerated $NiHPMo_{12}$ show (Figure 10) bands at 1065, 964, 879, 787 and 456 cm^{-1} corresponding to ν_{as}(P-O), ν_{as}(M=O_t), ν_{as}(Mo-O_b-Mo), ν_{as}(Mo-O_c-Mo) and ν_{as}(Ni-O) respectively, which is similar to the fresh catalyst

without exhibiting any significant shift. This indicates that the catalyst structure is intact even after regeneration. However, in terms of intensity, spectrum differs slightly from the fresh one, which may be due to the sticking of the substrates on the surface of regenerated catalyst.

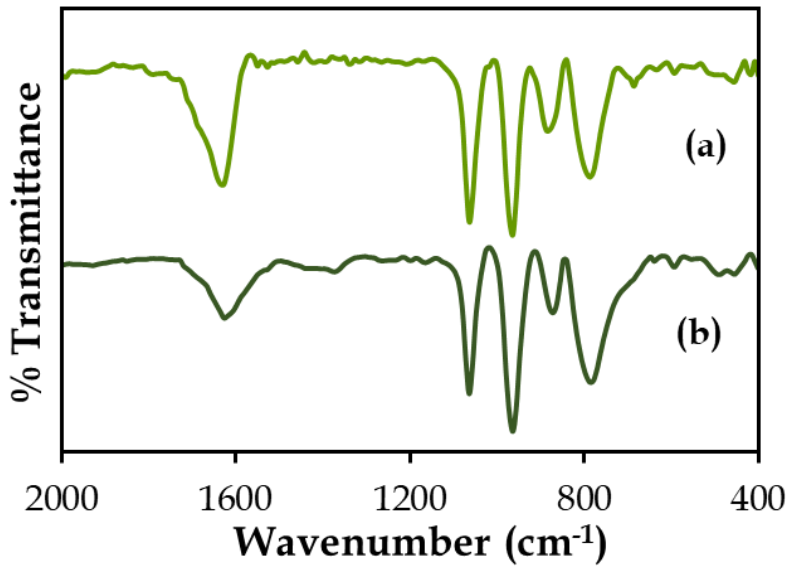

Figure 10. FT-IR of (a) fresh $NiHPMo_{12}$ and (b) regenerated $NiHPMo_{12}$

The UV-Vis spectra of regenerated catalyst was carried in aqueous phase and shows (Figure 11) d-d transition at 397 nm characteristic peaks for Ni(II). Also, LMCT charge transfer between O and Mo at 230 nm was observed, which is identical with fresh catalyst and confirms that the Keggin unit remains intact.

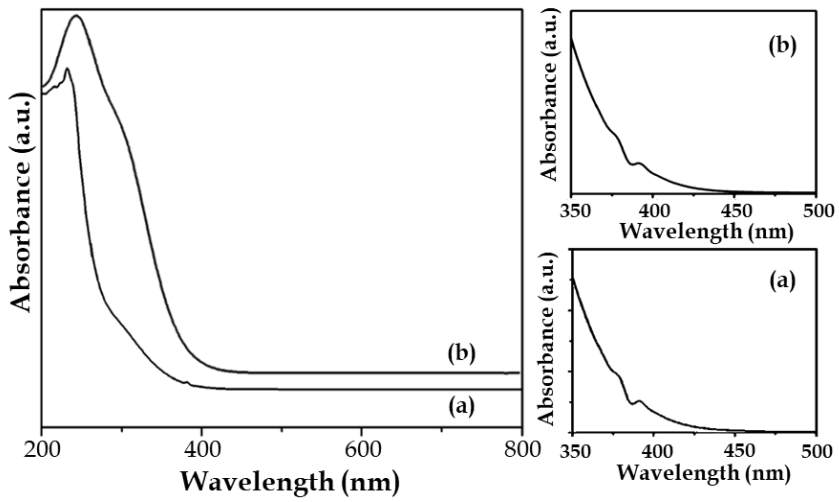

Figure 11. UV-Visible spectra of (a) fresh $NiHPMo_{12}$ and (b) regenerated $NiHPMo_{12}$

The X-ray photoelectron spectra of regenerated $NiHPMo_{12}$ is shown in figure 12. The obtained spectrum show intense peaks at 234, 236, 397 and 416 eV which correspond to $3d_{5/2}$, $3d_{3/2}$, $3p_{3/2}$ and $3p_{1/2}$ energy level of Mo(VI) and a low intense peak at 856 eV which corresponds to $2p_{1/2}$ of Ni(II) on the surface and are identical with fresh catalyst $NiHPMo_{12}$. This shows that the catalyst structure remains intact even after regeneration.

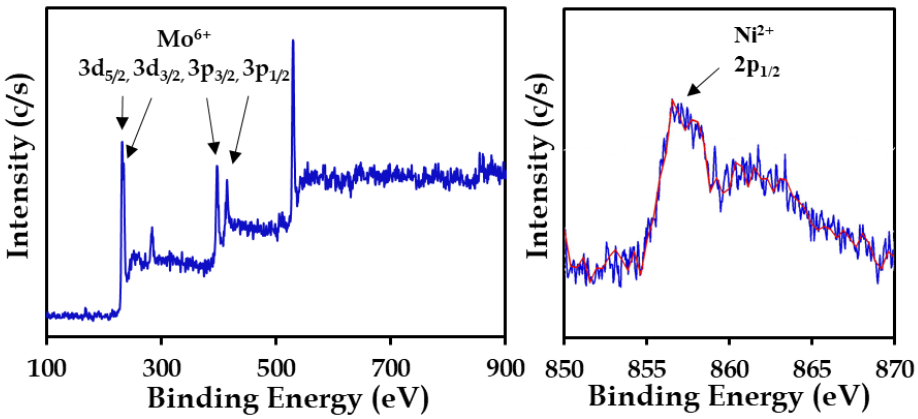

Figure 12. XPS spectra of regenerated $NiHPMo_{12}$

Mechanistic investigation

To confirm either the reaction proceeds via formation of acetal as intermediate according to a reported general reaction mechanism [38] or through benzoic acid as intermediate, earlier reported by our group [22, 36] the following set of reactions were carried out: i) when benzoic acid was used as a substrate under optimized condition (in absence of H_2O_2) yielding 45% conversion with 100% selectivity of methyl benzoate. ii) In another set of reaction, benzaldehyde was allowed to react with MeOH in presence of catalyst and absence of H_2O_2 yielding 15 % conversion with 76% selectivity of ester and 24% selectivity of benzoic acid. The reaction was prolonged for 3 h with addition of H_2O_2, yielding 50 % conversion as well as 69 % selectivity of ester. This study shows that oxidative esterification reaction proceeds through in situ generation of benzoic acid rather than an acetal intermediates.

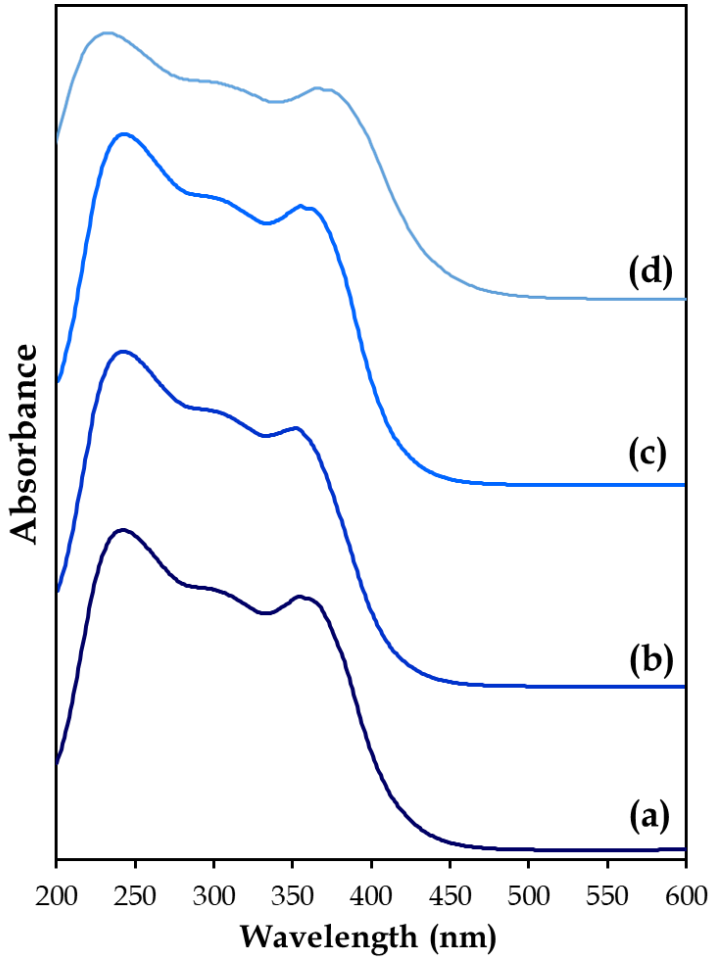

Figure 13. UV-Visible spectra of (a) Reaction starting point (b) after 3 h (c) after 6 h and (d) after 8 h

Here, in this paper, first time we attempted for more insight to understand the mechanistic aspects and for that the said reaction was monitored at different time intervals by UV-Vis and Raman spectroscopy (Figure 13 and 14). UV-Vis spectra of fresh $NiHPMo_{12}$ shows (Figure 3) two absorbance peaks at 230 and 396 nm due to ligand to metal charge transfer ($O^{2-} \rightarrow Mo^{6+}$) and d-d transition of Ni respectively [22, 26]. It is interesting to note that the formation of new absorbance peaks at 309 and 363 nm (Figure 13a) after the addition of H_2O_2 indicates the presence of oxo species of $Ni(O_2)$ [22] and peroxo species of $PO_4[MoO(O_2)_2]_4^{3-}$ [26] respectively, which are responsible for catalytic activity and are in good agreement with the reported one. UV-Vis spectrum were taken after 3 h (Figure 13b) as well as after 6 h (Figure 13c) and was found similar confirming the presence of active species. While after the completion of 8 hours

the disappearance of absorbance bands at 365 and 309 nm and reappearance of original peaks (Figure 13d) indicate that both, Ni and Mo play role for the mentioned reaction.

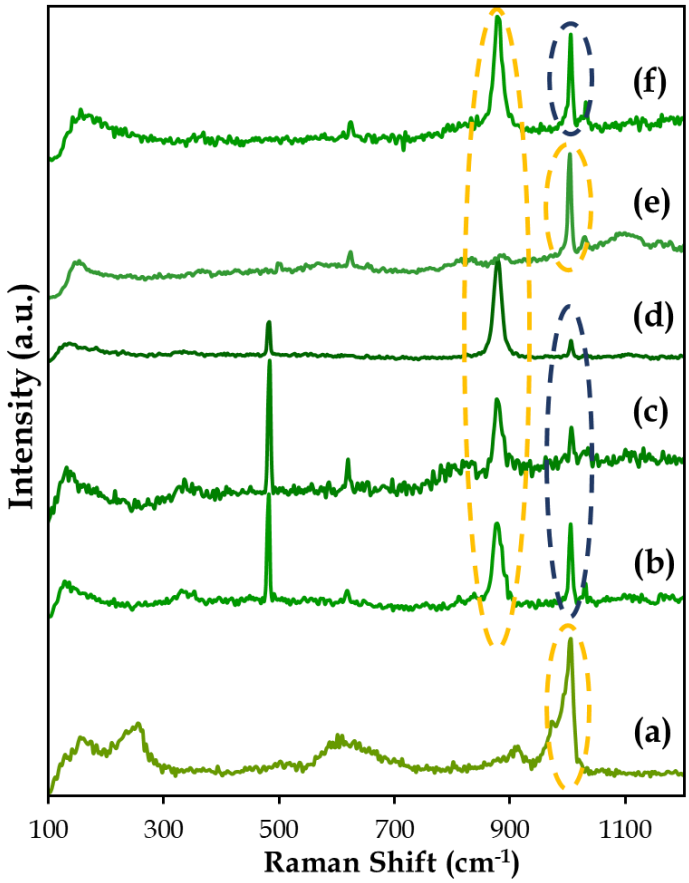

Figure 14. Raman spectra of (a) Fresh catalyst (b) Reaction starting (c) After 3 h (d) After 6 h (e) After 8 h and (f) After 8 h + H_2O_2

Further to confirm the above results, same reaction mixtures were studied by Raman spectroscopy. Unfortunately, we could not get any information about Ni oxo species due to very less concentration of active Ni (2.64×10^{-3} mmol). However, the study clearly shows that peroxo species of Mo played role for in-situ oxidation of Benzaldehyde to Benzoic acid. Figure 14 shows the Raman spectra of $NiHPMo_{12}$ at different time interval during the reaction. After the addition of H_2O_2, a new peak appears at 881 cm^{-1} (Figure 14b), which is a characteristic of $Mo(O_2)$ [26] with a less intense and slight shifting showing the formation of peroxo species immediately after addition of H_2O_2. With the

progress of the reaction the intensity of the Mo=O (1004 cm^{-1}) peak decreases (Figure 14c-d) with increase in the intensity of the $Mo(O_2)$ band due to the formation of more peroxo species. After completion of the reaction (Figure 14e), the original band of 1004 cm^{-1} (Mo=O) reappears. Further, in order to confirm the formation of peroxo species, H_2O_2 was once again added into the reaction mixture and we found the formation of a new band at 881 cm^{-1} (Figure 14f). Thus, the study confirms the formation of peroxo species during the reaction is because of H_2O_2. The following mechanism (scheme 3), is almost same as reported by our group earlier [22, 36]. It is known that for oxidation reactions involving polyoxometalates and transition metals, H_2O_2, first binds to the metal centre and then transfers an oxygen atom to the substrate. Thus, the activation of the metal centre results via the generation of the active species, peroxo species [39]. In the present case also, the formation of active metal-peroxo intermediate (where, metal is both, Mo as well as Ni) (Figure 13 and 14) is confirmed by UV-Vis and Raman spectroscopy studies. In the beginning of the reaction, $NiHPMo_{12}$ reacts with 30% H_2O_2 (v/v) to produce the active metal-peroxo intermediate-II, which is an active species for the insertion of benzaldehyde to form intermediate-III. Finally, MeOH directly reacts with intermediate-III and form product (Methyl benzoate) as shown in scheme 3 (Step-IV). It can be concluded that both Mo and Ni contributes simultaneously in terms of Mo-peroxo spices for oxidation while Ni-Oxo specie for esterification reaction.

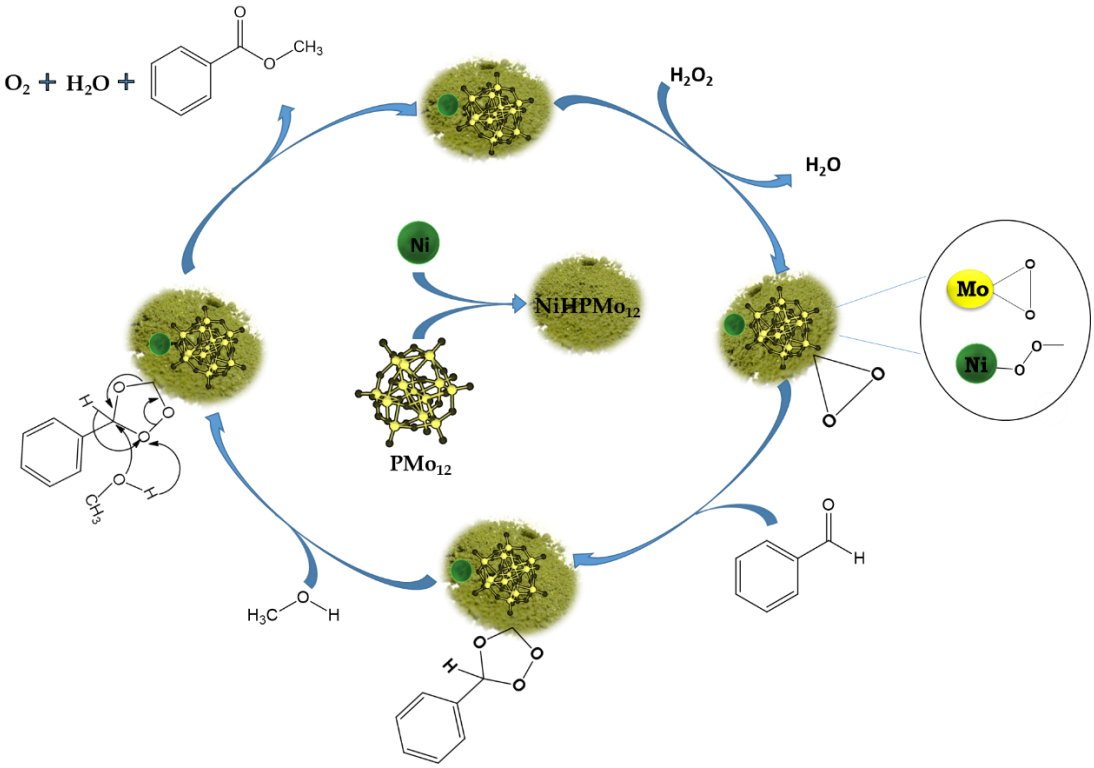

Scheme 3. Proposed reaction mechanism for oxidative esterification of benzaldehyde

Viability of the catalyst

To find reactivity of synthesized catalyst towards different aromatic aldehyde, the catalytic activity was carried out under optimized reaction condition and obtained results are shown in table 6. Study shows that the strong electron withdrawing group –Cl facilitates the reaction more as compared to –Br as expected. Aliphatic aldehyde also gives satisfactory conversions. This achieved result displays that the activity of synthesized catalyst with various substrates under mild reaction condition is outstanding.

Table 5. Substrate study

Sr.	Substrate	Product	%Conversion/ %Selectivity	TON
1	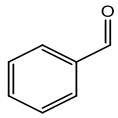	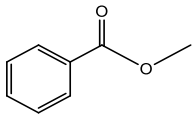	68/86	2576
2	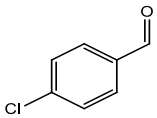	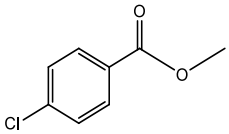	72/88	2711
3	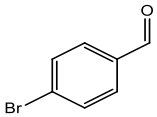	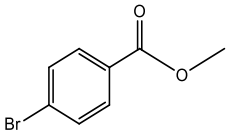	69/87	2590
4	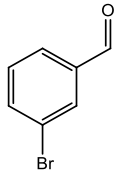	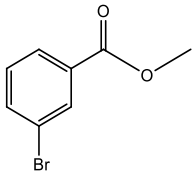	65/86	2447
5	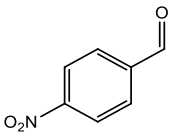	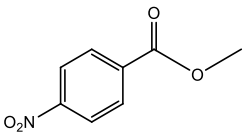	67/89	2522
6	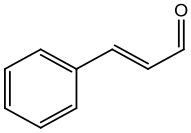	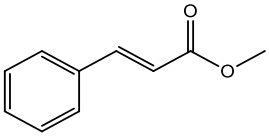	61/81	2296
7	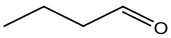	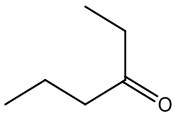	59/77	2221

Reaction condition: Catalyst amount (5 mg), Substrate (10 mmol), H_2O_2 (30 mmol, 30% v/v), MeOH (7 mL), temperature (80 ^{0}C) and time (6 h).

CONCLUSION

- **Bi-functional** catalytic activity of **Ni (Lewis acid)** and **Mo (Redox property)** was explored for conversion of **benzaldehyde to benzoate**.
- The catalyst gives **68% conversion with 86%** selectivity of ester using very small amount of **Ni (0.155 mg)** with **2576 TON**.
- Even though the catalyst is **homogeneous in nature**, it is **recyclable** and can be **reused** for a **number of cycles**.
- **Formation** as well as **role** of intermediates, **peroxo** and **oxo** species, were confirmed by **UV-Visible** and **Raman spectroscopy**.

REFERENCES

[1] V. Palermo, Á. G. Sathicq, T. Constantieux, J. Rodríguez, P. G. Vázquez, G. P. Romanelli, Catal. Lett., 146, 1634, (2016).

[2] G. Li, Y. Ding, J. Wang, X. Wang, J. Suo, J. Mol. Catal. A: Chem., 262, 67, (2007).

[3] M. Misono, Chem. Commun., 1141, (2001).

[4] Y. Yu, D. Sun, S. Wang, M. Xiao, L. Sun, Y. Meng, Catalysts, 9, 320, (2019).

[5] Y. Song, X. Wang, Y. Qu, C. Huang, Y. Li, B. Chen, Catalysts, 6, 49, 2016.

[6] A. Popa, V. Sasca, O. Verdes, A. Oszko, Catal. Today, 306, 233, (2018).

[7] Q. Huynh, Y. Schuurman, P. Delichere, S. Loridant, J. M. M. Millet, J. Catal., 261, 166, (2009).

[8] M. J. Darabi Mahboub, J. Wright, D. C. Boffito, J.-L. Dubois, G. S. Patience, Appl. Catal. A: Gen., 554, 105, (2018).

[9] A. Spojakina, E. Kraleva, K. Jiratova, L. Petrov, Appl. Catal. A: Gen., 288, 10-17, (2005).

[10] K. T. V. Rao, B. Haribabu, P. S. S. Prasad, N. Lingaiah, ChemCatChem, 4, 1173, (2012).

[11] I. H. Baek, P. Sharma, J. Porous Mater., 23, 1207, (2016).

[12] T. Al-Garni, N. Al-Jallal, A. Aouissi, J. Chem., 2017, 5641604, (2017).

[13] Q. Zhang, C. Yue, Q. Pu, T. Yang, Z. Wu, Y. Zhang, ACS Omega, 4, 9041, (2019).

[14] B. Demirel, E. N. Givens, Fuel Process. Technol., 64, 177, (2000).

[15] P. Blanchard, C. Lamonier, A. Griboval, E. Payen, Appl. Catal. A: Gen., 322, 33, (2007).

[16] A. Popa, V. Sasca, D. Bajuk-Bogdanović, I. Holclajtner-Antunović, J. Therm. Anal. Calorim, 126, 1567, (2016).

[17] G. A. Tsigdinos, Ind. Eng. Chem. Prod. Res. Dev., 13, 267, (1974).

[18] N. Mizuno, M. Tateishi, M. Iwamoto, J. Chem. Soc., Chem. Commun., 1411, (1994).

[19] T. Mazari, C. R. Marchal, S. Hocine, N. Salhi, C. Rabia, J. Nat. Gas Chem., 19, 54, (2010).

[20] A. Tahar, S. Benadji, T. Mazari, L. Dermeche, C. Marchal-Roch, C. Rabia, Catal. Lett., 145, 569, (2015).

[21] S. Mouanni, D. Amitouche, T. Mazari, C. Rabia, Appl. Petrochem. Res., 9, 67-75, (2019).

[22] S. Singh, A. Patel, P. Prakashan, Appl. Catal. A: Gen., 505, 131, (2015).

[23] A. Patel, S. Pathan, P. Prakashan, RSC Adv., 6, 51394, (2016).

[24] K. Jagadeeswaraiah, C. R. Kumar, P. S. S. Prasad, N. Lingaiah, Catal. Sci. Technol., 4, 2969, (2014).

[25] S. Kendell, T. Brown, React. Kinet. Mech. Catal., 99, 251, (2010).

[26] J. M. Brégeault, C. Aubry, G. Chottard, N. Platzer, F. Chauveau, C. Huet, H. Ledon, New insights into the catalytic activity of polyoxometalates for oxidation with hydrogen peroxide, in: L.I. Simándi (Ed.) Studies in Surface Science and Catalysis, Elsevierpp. 521, (1991).

[27] C. Rocchiccioli-Deltcheff, M. Amirouche, M. Fournier, J. Catal., 138, 445, (1992).

[28] A. J. Bridgeman, Chem. Phys., 287, 55, (2003).

[29] C. Rocchiccioli-Deltcheff, R. Thouvenot, R. Franck, Spectrochim. Acta A Mol., 32, 587, (1976).

[30] M. T. Pope, A. Müller, Polyoxometalate Chemistry From Topology via Self-Assembly to Applications, Springer Netherlands, (2001).

[31] A. Popa, V. Sasca, D. Bajuk-Bogdanović, I. Holclajtner-Antunović, J. Porous Mater., 23, 211, (2016).

[32] J. Xie, H. Zhang, S. Li, R. Wang, X. Sun, M. Zhou, J. Zhou, X. W. Lou, Y. Xie, Adv. Mater., 25, 5807, (2013).

[33] L. Zhao, J. Jia, Z. Yang, J. Yu, A. Wang, Y. Sang, W. Zhou, H. Liu, Appl. Catal. B: Environ., 210, 290, (2017).

[34] Z. Li, L. Mo, Y. Kathiraser, S. Kawi, ACS Catal., 4, 1526, (2014).

[35] J. Li, P. Li, J. Li, Z. Tian, F. Yu, Catalysts, 9, 506, 2019.

[36] A. Patel, A. Patel, RSC Adv., 9, 1460, (2019).

[37] E. Rafiee, S. Eavani, J. Mol. Catal. A: Chem., 373, 30, (2013).

[38] R. Tayebee, M. Fattahi Abdizadeh, B. Maleki, E. Shahri, J. Mol. Liq., 241, 447, (2017).

[39] S. T. Oyama, Mechanisms in Homogeneous and Heterogeneous Epoxidation Catalysis, Elsevier Science, (2011).

Published Papers

1. Nickel salt of phosphomolybdic acid as a bi-functional homogeneous recyclable catalyst for base free transformation of aldehyde into ester, Anjali Patel and **Jay Patel**, RSC Adv., 10, (2020) 22146-22155. https://doi.org/10.1039/D0RA04119J **[I. F. = 4.036]**
2. Cesium salt of iron substituted phosphomolybdate: Synthesis, characterization, room temperature hydrogenation of styrene and its mechanistic evaluation, Anjali Patel and **Jay Patel**, Mol. Catal., 513, (2021) 111827. https://doi.org/10.1016/j.mcat.2021.111827 **[I. F. = 5.089]**
3. Fe Exchanged Supported Phosphomolybdic Acid: Synthesis, Characterization and Low Temperature Water Mediated Hydrogenation of Cyclohexene, Anjali Patel and **Jay Patel**, Catalysis Letters, 152, (2022), 2716–2728. https://doi.org/10.1007/s10562-021-03838-8 **[I. F. = 3.186]**
4. Pd single-atom-site stabilized by supported phosphomolybdic acid: design, characterizations and tandem Suzuki–Miyaura cross coupling/nitro hydrogenation reaction, **Jay Patel and** Anjali Patel, Nanoscale Adv., 4, (2022) 4321-4334. https://doi.org/10.1021/acs.inorgchem.1c00636 **[I. F. = 5.598]**
5. Solvent free hydrogenation of Levulinic acid over in-situ generated Ni(0) stabilized by supported phosphomolybdic acid using formic acid as an internal hydrogen source, **Jay Patel and** Anjali Patel, **Renew. Energ. (Accepted)** **[I. F. = 8.634]**

Additional Publications

1. Chiral Phosphotungstate Functionalized with (S)-1- Phenylethylamine: Synthesis, Characterization, and Asymmetric Epoxidation of Styrene", Anjali Patel, Rajesh Sadasivan and **Jay Patel**, Inorg. Chem., 60, 15, (2021) 10979–10989. https://doi.org/10.1021/acs.inorgchem.1c00636 **[I. F. = 5.436]**

Papers presented

1. "A New Composite Materials Containing Iron and Phosphomolybdic acid: Synthesis, Characterization and Oxidation of Styrene"- **Virtual oral presentation** 3rd International Conference on Recent Advances in Material Chemistry (ICRAMC-2019), SRM Institute of Science and Technology, Kattankulathur, Chennai, February 13-15, 2019.
2. "Cs salt of Fe substituted phosphomolybdate catalysed aqueous phase hydrogenation reaction of Styrene"- **poster presentation** at International Conference on Advances in Catalysis: Industrial Outlook, CSIR-Indian Institute of Chemical Technology, Hyderabad, August 1 – 2, 2019.
3. "Fe substituted phosphomolybdate highly efficient versatile catalyst for hydrogenation and oxidation of styrene"- **poster presentation** at Second Virtual International Conference on Chemical Sciences in Sustainable Technology and Development (IC2S2TD-2021), November 24 -26, 2021.

Seminars/Workshops attended

1. National seminar on "Frontiers in Heterogeneous Catalysis" (HETCAT-2018), organized by Department of Chemistry, Faculty of Science, The Maharaja Sayajirao University of Baroda, Vadodara on December 8-9, 2018.
2. One day seminar on "Applications of X-Ray techniques- XRF, XPS, Auger" organized by Indian Society of Analytical Scientists, Baroda chapter and Department of Chemistry, Faculty of Science, The Maharaja Sayajirao University of Baroda, Vadodara on March 9, 2019
3. One day seminar on, "Analytical Instrumental Techniques" organized by Department of Environmental Studies, Faculty of Science, The Maharaja Sayajirao University of Baroda, Vadodara on April 9, 2019
4. One day workshop on, "Industrial Catalysis (ICAT-2019)" organized by Department of Chemistry, Faculty of Science, The Maharaja Sayajirao University of Baroda, Vadodara on November 23, 2019
5. Webinar on, "Infrared Spectroscopy with evolved gas analyzer" organized by Perkin Elmer, India on May 15, 2020